

\mathcal{BB} Intermeson Potentials in the Quark Model

T.Barnes,^{1,2*} N.Black,^{2†} D.J.Dean^{1,2‡} and E.S.Swanson^{3§}

¹*Physics Division, Oak Ridge National Laboratory,*

Oak Ridge, TN 37831-6373

²*Department of Physics and Astronomy, University of Tennessee*

Knoxville, TN 37996-1501

³*Department of Physics and Astronomy, North Carolina State University*

Raleigh, NC 27695-8202

Abstract

In this paper we derive quark model results for scattering amplitudes and equivalent low energy potentials for heavy meson pairs, in which each meson contains a heavy quark. This “ \mathcal{BB} ” system is an attractive theoretical laboratory for the study of the nuclear force between color singlets; the hadronic system is relatively simple, and there are lattice gauge theory (LGT) results for $V_{BB}(r)$ which may be compared to phenomenological models. We find that the quark model potential (after lattice smearing) has qualitative similarities to the LGT potential in the two B^*B^* channels in which direct comparison is possible, although there is evidence of a difference in length scales. The quark model prediction of equal magnitude

*email: barnes@orph01.phy.ornl.gov

†email: nblack@nomad.phys.utk.edu

‡email: dean@orph01.phy.ornl.gov

§email: swanson@unity.ncsu.edu

but opposite sign for $I=0$ and $I=1$ potentials also appears similar to LGT results at intermediate r . There may however be a discrepancy between the LGT and quark model $I=1$ BB potentials. A numerical study of the two-meson Schrödinger equations in the $(b\bar{q})(b\bar{q})$ and $(c\bar{q})(c\bar{q})$ sectors with the quark model potentials finds a single $\mathcal{B}\mathcal{B}$ “molecule”, in the $I=0$ BB^* sector. Binding in other channels might occur if the quark model forces are augmented by pion exchange.

I. INTRODUCTION

The origin of the residual strong force between hadrons is a complicated problem. Several distinct scattering mechanisms have been suggested as important contributors to interhadron forces, and it may be difficult to distinguish these experimentally. As an example, models of the NN force have been proposed which include t-channel meson exchanges, short-range quark-gluon interactions, intermediate s-channel excitation of Δ baryons, and various other effects. Comparisons with NN data alone may not determine the relative importance of these mechanisms, since one might find an unphysical parameter set that happens to describe the data well with a particular scattering mechanism, especially if there are many free parameters.

This complication is illustrated by a “confusion theorem” which notes that the two mechanisms most often assumed in models of the NN force, t-channel meson exchange and quark interchange, can easily be misidentified since they correspond to identical flavor flow. Both scattering mechanisms are of course present in nature, and the problem is to determine their relative importance as a function of separation. One can see that they are physically distinct because they represent scattering through intermediate states in different sectors of Hilbert space, one additional $q\bar{q}$ pair for meson exchange versus no extra pairs for quark interchange.

Lattice gauge theory provides an attractive opportunity to isolate the contributions

of the various mechanisms that have been proposed for residual interhadron forces. By taking the limit of a very heavy “ b ” quark and introducing sources for $\mathcal{B} = b\bar{q}$ mesons, one can study the energy of a meson pair as a function of separation [1–6]. (We follow [6] and use \mathcal{B} generically to refer both to a pseudoscalar B and a vector B^* ; technically $b\bar{q}$ is an anti- \mathcal{B} meson, but the results for scattering amplitudes and potentials are identical.) A lattice \mathcal{B} meson has a fixed heavy-quark coordinate, and in the $\mathcal{B}\mathcal{B}$ system one can use this to determine the energy $E_{\mathcal{B}\mathcal{B}}(r)$ of the $\mathcal{B}\mathcal{B}$ pair as a function of center-of-mass separation. The difference between this energy and that of two isolated \mathcal{B} mesons provides a natural definition of the $V_{\mathcal{B}\mathcal{B}}(r)$ interhadron potential. By changing the initial and final coordinates of the light-quark Green functions one can in effect vary the light quark flavor, and thereby determine the identical $\mathcal{B}\mathcal{B}$ (actually $I=1$) and distinguishable $\mathcal{B}\mathcal{B}$ ($I=0$) potentials. Changing the meson source angular quantum numbers allows one to infer separate BB , BB^* and B^*B^* potentials, providing that the associated multichannel mixing ambiguities can be resolved. One may also investigate the importance of different scattering mechanisms by evaluating potentials associated with different quark lines diagrams, such as direct versus quark interchange. Finally, in the more difficult full-QCD simulations one can test the importance of additional $q\bar{q}$ pairs in hadronic forces. Clearly, many questions which are of great importance to model builders may be answered by this application of lattice gauge theory.

In this paper we evaluate the various $\mathcal{B}\mathcal{B}$ potentials in the context of the nonrelativistic quark model, for comparison with existing and future LGT results. At present, configuration mixing in LGT constrains the direct comparison to two B^*B^* channels, but there is already evidence of qualitative agreement. Statistically more accurate LGT results and separation of the various B and B^* spin and isospin channels should allow very interesting comparisons with the various $\mathcal{B}\mathcal{B}$ potentials we derive here.

The paper is organised as follows: Section II introduces the Coulomb plus linear quark model and the technique used to evaluate hadron-hadron T-matrix elements, and

carries out the detailed evaluation with SHO wavefunctions. Section III gives the general relation between the T-matrix and equivalent local potentials, and uses this to derive the \mathcal{BB} potentials. Section IV discusses the details of these \mathcal{BB} quark model potentials and compares these to LGT results, and studies the possible formation of bound states using the \mathcal{BB} Schrödinger equation. Finally, Section V gives a summary and conclusions.

II. \mathcal{BB} T-MATRIX FROM THE QUARK-GLUON INTERACTION

A. Method and previous applications

The technique we use to determine quark model $V_{\mathcal{BB}}(r)$ potentials is to evaluate the lowest (Born) order T-matrix element of the interquark Hamiltonian between two-meson scattering states, which is then Fourier transformed to give an equivalent low-energy potential. The interaction assumed is the OGE color Coulomb and spin-spin interaction and linear scalar confinement. The effective interquark hamiltonian for this interaction is

$$H_I = \sum_{ij} \left\{ \left[\sum_a \mathcal{F}^a(i) \mathcal{F}^a(j) \right] \left[\frac{\alpha_s}{r_{ij}} - \frac{8\pi\alpha_s}{3m_i m_j} \vec{S}_i \cdot \vec{S}_j \delta(\vec{r}_{ij}) - \frac{3b}{4} r_{ij} \right] \right\}, \quad (1)$$

where the sum runs over all pairs (i, j) of valence quarks and antiquarks that are in different initial hadrons. (Pairs of quarks in the same hadron contribute to hadron energies rather than to scattering; the partition of H into H_0 and H_I in this formalism is well-known in atomic physics, and is discussed elsewhere in the hadronic context [7,8].) The color generator in H_I is as usual $\mathcal{F}^a = \lambda^a/2$ for quarks and $\mathcal{F}^a = -\lambda^{aT}/2$ for antiquarks. After a single interaction of this H_I between a constituent pair in different initial hadrons, quark line interchange is required to give an overlap with the color-singlet final meson states. For meson-meson scattering this gives four diagrams, which are shown in Fig.1.

This model (incorporating only the spin-spin OGE term, which is dominant in light hadrons) gives an excellent description of S-wave meson-meson scattering in channels without valence annihilation, specifically I=2 $\pi\pi$ [7] and I=3/2 $K\pi$ [9], with 2 and 3 parameters respectively $(\alpha_s/m_q^2, \beta_{SHO}; m_q/m_s)$. These successful results are impressive in

that the parameter values are already well known from light meson spectroscopy, and the optimum values found in fitting the scattering data alone are consistent. This suggests that, at least for $PsPs$ scattering at moderate energies, Born-order quark-gluon diagrams with external meson wavefunctions describe the dominant scattering mechanism. KN S-wave scattering at low momenta is also excellently described by this model. (A good simultaneous fit to higher-momentum S-wave KN scattering however requires a somewhat reduced nucleon wavefunction length scale [10]; this may be due to short-distance correlations in the nucleon's three-quark wavefunction, which is not included in our simple Gaussian forms.) In all these successfully modelled reactions there is of course no one-pion-exchange term, since a three-pseudoscalar vertex is not allowed. There are also no s-channel resonance contributions; these specific reactions were studied precisely because they do not have the complication of valence $q\bar{q}$ annihilation. Studies of the NN interaction in the quark model [11], using both perturbative and nonperturbative techniques, have found a large short-range repulsive NN core interaction due to this OGE interaction, and similarly conclude that the dominant core interaction at short distances arises from the OGE spin-spin hyperfine term.

B. Evaluation of BB scattering amplitudes

In this paper we evaluate the contribution of all three terms in Eq.(1) to the BB T-matrix elements $\{T_{fi}\}$ and potentials $\{V_{BB}(r)\}$. These will be presented with separate flavor, color, spin and space factors, so the BB case can easily be generalized to other \mathcal{BB} spin channels. Although the spin-spin hyperfine term was found to be dominant in light pseudoscalar-pseudoscalar S-wave scattering, in BB we also expect the color Coulomb interaction to be important, since it must dominate at short distances. We will derive the $\{T_{fi}\}$ for general quark masses, with \bar{m} the light (antiquark) mass and m the heavy “ b quark” mass.

To evaluate the meson-meson potential we first calculate the matrix element of the

quark Hamiltonian Eq.(1) between two-meson initial and final states. Conservation of three-momentum implies that this matrix element is of the form

$$\langle CD|H_I|AB\rangle = \frac{1}{(2\pi)^3} T_{fi} \delta(\vec{A} + \vec{B} - \vec{C} - \vec{D}) . \quad (2)$$

(In previous scattering calculations we instead gave results for a Hamiltonian matrix element h_{fi} , which is trivially related to the Born-order T-matrix element by $h_{fi} = T_{fi}/(2\pi)^3$.) In our earlier discussion of $\pi\pi$ scattering [7] we distinguished the four scattering diagrams according to which pair of constituents interacted; these are “capture₁” (C1), “capture₂” (C2), “transfer₁” (T1) and “transfer₂” (T2); see Fig.1. The hadron-hadron T_{fi} matrix element for each diagram can conveniently be written as an overlap integral of the meson wavefunctions times the underlying quark-level T-matrix element.

In the quark-quark T_{fi} (Fig.2) the initial and final constituent momenta are $\vec{a}, \vec{b} \rightarrow \vec{a}', \vec{b}'$. It is useful to write the quark-quark T_{fi} in terms of the linear combinations \vec{q}, \vec{p}_1 and \vec{p}_2 , defined by $\vec{q} = \vec{a}' - \vec{a} = \vec{b} - \vec{b}'$, $\vec{p}_1 = (\vec{a} + \vec{a}')/2$ and $\vec{p}_2 = (\vec{b} + \vec{b}')/2$. For the specific case of one gluon exchange, the complete quark-quark T_{fi} to second-order in three-momenta (suppressing the color factor) is

$$\begin{aligned} T_{fi}^{OGE}(\vec{q}, \vec{p}_1, \vec{p}_2) = & 4\pi\alpha_s \left[\frac{1}{\vec{q}^2} - \frac{1}{8m_1^2} - \frac{1}{8m_2^2} + \frac{i}{2\vec{q}^2} \left(\frac{1}{m_1^2} \vec{S}_1 \cdot (\vec{q} \times \vec{p}_1) - \frac{1}{m_2^2} \vec{S}_2 \cdot (\vec{q} \times \vec{p}_2) \right) \right. \\ & - \frac{2}{3m_1m_2} \vec{S}_1 \cdot \vec{S}_2 + \frac{1}{m_1m_2\vec{q}^2} \left(\vec{S}_1 \cdot \vec{q} \vec{S}_2 \cdot \vec{q} - \frac{\vec{q}^2}{3} \vec{S}_1 \cdot \vec{S}_2 \right) - \frac{i}{m_1m_2\vec{q}^2} \left(\vec{S}_1 \cdot (\vec{q} \times \vec{p}_2) - \vec{S}_2 \cdot (\vec{q} \times \vec{p}_1) \right) \\ & \left. - \frac{1}{m_1m_2\vec{q}^2} \left(\vec{p}_1 \cdot \vec{p}_2 - \frac{1}{\vec{q}^2} \vec{p}_1 \cdot \vec{q} \vec{p}_2 \cdot \vec{q} \right) \right] . \quad (3) \end{aligned}$$

This follows from taking the matrix element the one-gluon-exchange effective hamiltonian $j^\mu \Delta^{\mu\nu} j^\nu$ between an initial and final quark pair, and using the definition Eq.(2) of T_{fi} . We have displayed the $\gamma_0\gamma_0$ terms and the $\gamma_i\gamma_i$ terms separately in this T_{fi} ; the $\gamma_i\gamma_i$ terms are proportional to $1/m_1m_2$. This result is valid for both quarks and antiquarks; only the color factor distinguishes them. For completeness we give the corresponding T-matrix element due to linear scalar confinement, which is

$$T_{fi}^{lin.}(\vec{q}, \vec{p}_1, \vec{p}_2) = \frac{6\pi b}{\vec{q}^4} \left[1 - \frac{1}{2} \left(\frac{\vec{p}_1^2}{m_1^2} + \frac{\vec{p}_2^2}{m_2^2} \right) - \frac{i}{2} \left(\frac{1}{m_1^2} \vec{S}_1 \cdot (\vec{q} \times \vec{p}_1) - \frac{1}{m_2^2} \vec{S}_2 \cdot (\vec{q} \times \vec{p}_2) \right) \right]. \quad (4)$$

In the four overlap integrals that result from taking the two-meson matrix elements of these quark T-matrices (corresponding to the four independent scattering diagrams) we find that \vec{p}_2 is constrained to equal $\pm\vec{p}_1$ plus a diagram-dependent shift. These overlap integrals are explicitly (introducing $\lambda \equiv (m - \bar{m})/(m + \bar{m})$, and using $\vec{p} \equiv \vec{p}_1$ as an integration variable)

$$T_{fi}^{(C1)}(AB \rightarrow CD) = \iint d^3q d^3p \Phi_C^*(2\vec{p} + \vec{q} - (1 + \lambda)\vec{C}) \Phi_D^*(2\vec{p} - \vec{q} - 2\vec{A} - (1 - \lambda)\vec{C}) T_{fi}(\vec{q}, \vec{p}, -\vec{p} + \vec{C}) \Phi_A(2\vec{p} - \vec{q} - (1 + \lambda)\vec{A}) \Phi_B(2\vec{p} - \vec{q} - (1 - \lambda)\vec{A} - 2\vec{C}), \quad (5)$$

$$T_{fi}^{(C2)}(AB \rightarrow CD) = \iint d^3q d^3p \Phi_C^*(-2\vec{p} + \vec{q} + 2\vec{A} - (1 + \lambda)\vec{C}) \Phi_D^*(-2\vec{p} - \vec{q} - (1 - \lambda)\vec{C}) T_{fi}(\vec{q}, \vec{p}, -\vec{p} - \vec{C}) \Phi_A(-2\vec{p} + \vec{q} + (1 - \lambda)\vec{A}) \Phi_B(-2\vec{p} + \vec{q} + (1 + \lambda)\vec{A} - 2\vec{C}), \quad (6)$$

$$T_{fi}^{(T1)}(AB \rightarrow CD) = \iint d^3q d^3p \Phi_C^*(2\vec{p} + \vec{q} - (1 + \lambda)\vec{C}) \Phi_D^*(2\vec{p} - \vec{q} - 2\vec{A} - (1 - \lambda)\vec{C}) T_{fi}(\vec{q}, \vec{p}, \vec{p} - \vec{A} - \vec{C}) \Phi_A(2\vec{p} - \vec{q} - (1 + \lambda)\vec{A}) \Phi_B(2\vec{p} + \vec{q} - (1 - \lambda)\vec{A} - 2\vec{C}), \quad (7)$$

$$T_{fi}^{(T2)}(AB \rightarrow CD) = \iint d^3q d^3p \Phi_C^*(-2\vec{p} + \vec{q} + 2\vec{A} - (1 + \lambda)\vec{C}) \Phi_D^*(-2\vec{p} - \vec{q} - (1 - \lambda)\vec{C}) T_{fi}(\vec{q}, \vec{p}, \vec{p} - \vec{A} + \vec{C}) \Phi_A(-2\vec{p} + \vec{q} + (1 - \lambda)\vec{A}) \Phi_B(-2\vec{p} - \vec{q} + (1 + \lambda)\vec{A} - 2\vec{C}). \quad (8)$$

With standard quark model SHO wavefunctions (given in Appendix A) each overlap integral above becomes the quark T_{fi} times a shifted Gaussian. The overlap integrals are then (also assuming elastic scattering in the CM frame, so $|\vec{A}| = |\vec{C}|$)

$$T_{fi}^{(C1)}(AB \rightarrow CD) = \frac{1}{\pi^3 \beta^6} \exp \left\{ -\frac{1}{3\beta^2} [(1+\lambda)^2 \vec{A}^2 - 2\lambda(\vec{A}^2 + \vec{A} \cdot \vec{C})] \right\} \\ \iint d^3q d^3p \exp \left\{ -\frac{2}{\beta^2} (\vec{p} - \vec{p}_0)^2 \right\} \exp \left\{ -\frac{3}{8\beta^2} (\vec{q} - \vec{q}_0)^2 \right\} T_{fi}(\vec{q}, \vec{p}, -\vec{p} + \vec{C}), \quad (9)$$

$$T_{fi}^{(C2)}(AB \rightarrow CD) = \frac{1}{\pi^3 \beta^6} \exp \left\{ -\frac{1}{3\beta^2} [(1+\lambda)^2 \vec{A}^2 - 2\lambda(\vec{A}^2 + \vec{A} \cdot \vec{C})] \right\} \\ \iint d^3q d^3p \exp \left\{ -\frac{2}{\beta^2} (\vec{p} - \vec{p}_0)^2 \right\} \exp \left\{ -\frac{3}{8\beta^2} (\vec{q} - \vec{q}_0)^2 \right\} T_{fi}(\vec{q}, \vec{p}, -\vec{p} - \vec{C}), \quad (10)$$

$$T_{fi}^{(T1)}(AB \rightarrow CD) = \frac{1}{\pi^3 \beta^6} \exp \left\{ -\frac{1}{4\beta^2} [(1-\lambda)^2 (\vec{A}^2 + \vec{A} \cdot \vec{C})] \right\} \\ \iint d^3q d^3p \exp \left\{ -\frac{2}{\beta^2} (\vec{p} - \vec{p}_0)^2 \right\} \exp \left\{ -\frac{1}{2\beta^2} (\vec{q} - \vec{q}_0)^2 \right\} T_{fi}(\vec{q}, \vec{p}, \vec{p} - \vec{A} - \vec{C}), \quad (11)$$

$$T_{fi}^{(T2)}(AB \rightarrow CD) = \frac{1}{\pi^3 \beta^6} \exp \left\{ -\frac{1}{4\beta^2} [(1+\lambda)^2 (\vec{A}^2 - \vec{A} \cdot \vec{C})] \right\} \\ \iint d^3q d^3p \exp \left\{ -\frac{2}{\beta^2} (\vec{p} - \vec{p}_0)^2 \right\} \exp \left\{ -\frac{1}{2\beta^2} (\vec{q} - \vec{q}_0)^2 \right\} T_{fi}(\vec{q}, \vec{p}, \vec{p} - \vec{A} + \vec{C}). \quad (12)$$

The shifts \vec{p}_0 and \vec{q}_0 are diagram dependent, and are

$$\vec{p}_0 = \begin{cases} \vec{q}/4 + (\vec{A} + \vec{C})/2, & \text{C1} \\ \vec{q}/4 + (\vec{A} - \vec{C})/2, & \text{C2} \\ (\vec{A} + \vec{C})/2, & \text{T1} \\ (\vec{A} - \vec{C})/2, & \text{T2,} \end{cases} \quad (13)$$

$$\vec{q}_0 = \begin{cases} 2(-\vec{A} + \lambda\vec{C})/3, & \text{C1 and C2} \\ (1+\lambda)(-\vec{A} + \vec{C})/2, & \text{T1} \\ -(1-\lambda)(\vec{A} + \vec{C})/2, & \text{T2.} \end{cases} \quad (14)$$

Note that the C1 and C2 integrals over \vec{p} must be carried out before the \vec{q} integral, since the \vec{p}_0 shift depends explicitly on \vec{q} in this case.

These results are for a general quark $T_{fi}(\vec{q}, \vec{p}_1, \vec{p}_2)$. In this paper we consider the special case of \vec{p}_i -independent quark interactions, corresponding to pure $V(r_{ij})$ quark potentials in coordinate space. This simplification is appropriate for the color Coulomb, linear scalar confinement and spin-spin contact hyperfine interactions treated here; the spin-spin hyperfine term simply has an additional multiplicative spin factor for each diagram.

This assumption is not valid for the spin-orbit and tensor interactions, which have explicit \vec{p} dependence; these will be treated in subsequent work. Given a quark T-matrix of the form

$$T_{fi}(\vec{q}, \vec{p}_1, \vec{p}_2) = T_{fi}(\vec{q}) \quad (15)$$

we can further simplify the SHO overlap integrals above. This gives

$$\begin{aligned} T_{fi}^{(C1)}(AB \rightarrow CD) &= \frac{1}{(2\pi)^{3/2}\beta^3} \exp \left\{ -\frac{1}{3\beta^2} \left[(1+\lambda)^2 \vec{A}^2 - 2\lambda(\vec{A}^2 + \vec{A} \cdot \vec{C}) \right] \right\} \\ &\cdot \int d^3q \exp \left\{ -\frac{3}{8\beta^2} (\vec{q} - \vec{q}_0)^2 \right\} T_{fi}(\vec{q}) , \end{aligned} \quad (16)$$

$$T_{fi}^{(C2)}(AB \rightarrow CD) = T_{fi}^{(C1)}(AB \rightarrow CD) , \quad (17)$$

$$\begin{aligned} T_{fi}^{(T1)}(AB \rightarrow CD) &= \frac{1}{(2\pi)^{3/2}\beta^3} \exp \left\{ -\frac{1}{4\beta^2} \left[(1-\lambda)^2 (\vec{A}^2 + \vec{A} \cdot \vec{C}) \right] \right\} \\ &\cdot \int d^3q \exp \left\{ -\frac{1}{2\beta^2} (\vec{q} - \vec{q}_0)^2 \right\} T_{fi}(\vec{q}) , \end{aligned} \quad (18)$$

$$\begin{aligned} T_{fi}^{(T2)}(AB \rightarrow CD) &= \frac{1}{(2\pi)^{3/2}\beta^3} \exp \left\{ -\frac{1}{4\beta^2} \left[(1+\lambda)^2 (\vec{A}^2 - \vec{A} \cdot \vec{C}) \right] \right\} \\ &\cdot \int d^3q \exp \left\{ -\frac{1}{2\beta^2} (\vec{q} - \vec{q}_0)^2 \right\} T_{fi}(\vec{q}) \end{aligned} \quad (19)$$

where \vec{q}_0 for each diagram is given by Eq.(14).

C. Explicit meson-meson T-matrix elements

We will now evaluate these overlap integrals with the quark T_{fi} due to color Coulomb, spin-spin hyperfine and scalar confinement interactions, in Eq.(3) and Eq.(4) and transform these into equivalent low-energy V_{BB} potentials. The specific quark interactions we use are (with color and spin factors removed)

$$T_{fi}(\vec{q}) = \begin{cases} 4\pi\alpha_s/\vec{q}^2, & \text{color Coulomb} \\ -(8\pi\alpha_s/3m_i m_j), & \text{spin-spin hyperfine} \\ 6\pi b/\vec{q}^4, & \text{linear confinement.} \end{cases} \quad (20)$$

1. Spin-spin Hyperfine Contribution

The spin-spin hyperfine contribution is derived using the overlap integrals above and the color and spin matrix elements given in our previous discussion of I=2 $\pi\pi$ scattering [7]. The results are presented as the meson-meson T-matrix element $T_{fi}^{(\text{diagram})}(AB \rightarrow CD) = (\text{signature}) \cdot (\text{flavor factor}) \cdot (\text{color factor}) \cdot (\text{spin factor}) \cdot [\text{space overlap}]$. We also define a frequently occurring combination

$$\Pi^2 \equiv (1 - \lambda)^2(\vec{A} + \vec{C})^2 + (1 + \lambda)^2(\vec{A} - \vec{C})^2. \quad (21)$$

The results are

$$T_{fi}^{(\text{C1})} = (-1) \cdot (1) \cdot (-4/9) \cdot (-3/8) \cdot \left[-\frac{2^6\pi\alpha_s}{3^{5/2}m\bar{m}} \exp\left\{-\frac{\Pi^2}{12\beta^2}\right\} \right], \quad (22)$$

$$T_{fi}^{(\text{C2})} = T_{fi}^{(\text{C1})}, \quad (23)$$

$$T_{fi}^{(\text{T1})} = (-1) \cdot (1) \cdot (+4/9) \cdot (3/8) \cdot \left[-\frac{2^3\pi\alpha_s}{3m^2} \exp\left\{-\frac{(1-\lambda)^2}{8\beta^2}(\vec{A} + \vec{C})^2\right\} \right], \quad (24)$$

$$T_{fi}^{(\text{T2})} = (-1) \cdot (1) \cdot (+4/9) \cdot (3/8) \cdot \left[-\frac{2^3\pi\alpha_s}{3\bar{m}^2} \exp\left\{-\frac{(1+\lambda)^2}{8\beta^2}(\vec{A} - \vec{C})^2\right\} \right]. \quad (25)$$

2. Color Coulomb Contribution

The four color Coulomb overlap integrals can be evaluated similarly using the quark color Coulomb T_{fi} in Eq.(20), which gives the results

$$T_{fi}^{(\text{C1})} = (-1) \cdot (1) \cdot (-4/9) \cdot (1/2) \cdot \left[\frac{2^3\pi\alpha_s}{3^{1/2}\beta^2} {}_1F_1\left(1/2, 3/2; \frac{\Pi^2}{24\beta^2}\right) \exp\left\{-\frac{\Pi^2}{8\beta^2}\right\} \right], \quad (26)$$

$$T_{fi}^{(\text{C2})} = T_{fi}^{(\text{C1})}, \quad (27)$$

$$T_{fi}^{(\text{T1})} = (-1) \cdot (1) \cdot (4/9) \cdot (1/2) \cdot \left[\frac{2^2\pi\alpha_s}{\beta^2} {}_1F_1\left(1/2, 3/2; \frac{(1+\lambda)^2}{8\beta^2}(\vec{A} - \vec{C})^2\right) \exp\left\{-\frac{\Pi^2}{8\beta^2}\right\} \right], \quad (28)$$

$$T_{fi}^{(\text{T2})} = (-1) \cdot (1) \cdot (4/9) \cdot (1/2) \cdot \left[\frac{2^2\pi\alpha_s}{\beta^2} {}_1F_1\left(1/2, 3/2; \frac{(1-\lambda)^2}{8\beta^2}(\vec{A} + \vec{C})^2\right) \exp\left\{-\frac{\Pi^2}{8\beta^2}\right\} \right]. \quad (29)$$

TABLE I. Physically Allowed \mathcal{BB} States.

System		Angular Quantum Numbers		
mesons	I_{tot}	$S_{tot} = 0$	$S_{tot} = 1$	$S_{tot} = 2$
BB	1	even L	-	-
	0	odd L	-	-
BB^*	1	-	all L	-
	0	-	all L	-
B^*B^*	1	even L	odd L	even L
	0	odd L	even L	odd L

3. Scalar Confinement Contribution

Finally, with the linear scalar confinement T_{fi} we find

$$T_{fi}^{(C1)} = (-1) \cdot (1) \cdot (-4/9) \cdot (1/2) \cdot \left[-\frac{3^{3/2}\pi b}{\beta^4} {}_1F_1\left(-1/2, 3/2; \frac{\Pi^2}{24\beta^2}\right) \exp\left\{-\frac{\Pi^2}{8\beta^2}\right\} \right], \quad (30)$$

$$T_{fi}^{(C2)} = T_{fi}^{(C1)}, \quad (31)$$

$$T_{fi}^{(T1)} = (-1) \cdot (1) \cdot (4/9) \cdot (1/2) \cdot \left[-\frac{6\pi b}{\beta^4} {}_1F_1\left(-1/2, 3/2; \frac{(1+\lambda)^2}{8\beta^2}(\vec{A} - \vec{C})^2\right) \exp\left\{-\frac{\Pi^2}{8\beta^2}\right\} \right], \quad (32)$$

$$T_{fi}^{(T2)} = (-1) \cdot (1) \cdot (4/9) \cdot (1/2) \cdot \left[-\frac{6\pi b}{\beta^4} {}_1F_1\left(-1/2, 3/2; \frac{(1-\lambda)^2}{8\beta^2}(\vec{A} + \vec{C})^2\right) \exp\left\{-\frac{\Pi^2}{8\beta^2}\right\} \right]. \quad (33)$$

D. T-matrix elements for physical \mathcal{BB} states

Since the BB and B^*B^* systems have identical mesons there are constraints on the physically allowed states; these are summarized in Table I. The physical \mathcal{BB} scattering amplitudes are diagonal in isospin, since we have assumed equal light quark masses. To extract these isospin-diagonal amplitudes we evaluate the T-matrix element between

BB pairs with definite isospin, for example $|B^-B^- \rangle$ for $I=1$. With our phases the \bar{B} (b) and B (\bar{b}) meson isodoublets are $\{|\bar{B}^0\rangle, |B^- \rangle\} = \{-|b\bar{d}\rangle, |b\bar{u}\rangle\}$ and $\{|B^+\rangle, |B^0\rangle\} = \{-|u\bar{b}\rangle, -|d\bar{b}\rangle\}$, analogous to the kaon system. Since $|B^-B^- \rangle = |(b\bar{u})(b\bar{u})\rangle$, this implies identical antiquarks as well as quarks. As noted in Ref. [7], in this case there is a second set of ‘‘symmetrizing’’ quark line diagrams, with quark lines exchanged rather than antiquark lines. These have the effect of interchanging the final mesons C and D ; when added to the antiquark exchange diagrams of the previous section this gives a Bose-symmetric scattering amplitude, satisfying the even- L constraint in Table I. For BB (or $\bar{B}\bar{B}$) the complete $I=1$ BB elastic scattering amplitude is then

$$T_{fi}^{BB (I=1)} = T_{fi}(AB \rightarrow CD) + T_{fi}(AB \rightarrow DC) , \quad (34)$$

where $T_{fi}(AB \rightarrow CD)$ is the sum of Eqs.(22-33) of the previous section. Similarly for $I=0$ BB we find a second, symmetrizing diagram, but with an opposite sign;

$$T_{fi}^{BB (I=0)} = -T_{fi}(AB \rightarrow CD) + T_{fi}(AB \rightarrow DC) . \quad (35)$$

This gives a spatially antisymmetric scattering amplitude. Thus $I=1$ BB is allowed only even L and $I=0$ BB is allowed only odd L . Another consequence of the relative signs in $T_{fi}^{BB (I=0,1)}$ above is the relation between Born-order \mathcal{BB} potentials in systems that differ only in total isospin,

$$V_{\mathcal{BB}}^{(I=0)}(r) = -V_{\mathcal{BB}}^{(I=1)}(r) . \quad (36)$$

III. $V_{\mathcal{BB}}$ POTENTIALS

A. Potentials from the T-matrix: general formalism

A $2 \rightarrow 2$ T-matrix can be represented as an equivalent Born-order potential operator $V_{op.}(\vec{x}_1 - \vec{x}_2, \nabla_1, \nabla_2)$, between pointlike particles [12]. The definition of this potential operator is

$$\delta(\vec{A} + \vec{B} - \vec{C} - \vec{D}) T_{fi}(\vec{A}, \vec{B}, \vec{C}, \vec{D}) =$$

$$\frac{1}{(2\pi)^3} \iint d^3x_1 d^3x_2 e^{-i(\vec{C}\cdot\vec{x}_1 + \vec{D}\cdot\vec{x}_2)} V_{op}(\vec{x}_1 - \vec{x}_2, \nabla_1, \nabla_2) e^{+i(\vec{A}\cdot\vec{x}_1 + \vec{B}\cdot\vec{x}_2)}. \quad (37)$$

To evaluate this potential operator for a given T-matrix one can write the meson-meson $T_{fi}(AB \rightarrow CD)$ as a function of the variables $\vec{Q} = (\vec{C} - \vec{A})$, $\vec{P}_1 = (\vec{A} + \vec{C})/2$ and $\vec{P}_2 = (\vec{B} + \vec{D})/2$. A power series expansion in the $\{\vec{P}_i\}$ variables is then performed,

$$T_{fi}(AB \rightarrow CD) = T^{(0)}(\vec{Q}) + T_i^{(1,0)}(\vec{Q}) P_{1i} + T_i^{(0,1)}(\vec{Q}) P_{2i} + T_{ij}^{(1,1)}(\vec{Q}) P_{1i} P_{2j} + \dots \quad (38)$$

The $\{P_i\}$ in the T-matrix expansion are replaced by left- and right-gradients in the equivalent potential operator defined implicitly by Eq.(37). This procedure gives a local potential operator that reproduces the specified scattering amplitude T_{fi} at Born order. One may confirm that this approach reproduces the full $O(v^2/c^2)$ Breit-Fermi Hamiltonian when applied to the one photon exchange $e^-e^- T_{fi}$, expanded to $O(P_i^2)$.

The *leading* term $T^{(0)}(\vec{Q})$ in the P_i expansion is a function of \vec{Q} only, and Fourier transforms into a local (static limit) potential that is a function of $\vec{x}_1 - \vec{x}_2 = \vec{r}$ only. In the cases we consider here $T^{(0)}(\vec{Q})$ is a function of $|\vec{Q}|$ only, which leads to a local potential that is a function of r only. The relation between $T_{fi}(\vec{Q})$ and $V(\vec{r})$ is

$$V(\vec{r}) = \frac{1}{(2\pi)^3} \int d^3Q T^{(0)}(\vec{Q}) e^{i\vec{Q}\cdot\vec{r}}. \quad (39)$$

In this paper we obtain a local $V_{BB}(r)$ potential by Fourier transforming the $BB \rightarrow BB$ $T^{(0)}(\vec{Q})$, which we obtain from the full meson-meson T_{fi} by changing to the variables $\{\vec{Q}, \vec{P}_i\}$ and setting $\vec{P}_1 = \vec{P}_2 = 0$.

B. V_{BB} : individual contributions

1. Color Coulomb

As an illustration we shall evaluate the I=1 BB potential due to the color Coulomb interaction in the infinite m limit ($\lambda = 1$), following which we will simply quote the re-

maining results. The I=1 $B^- B^- T_{fi}$ matrix element we find for $\lambda = 1$ with this interaction is

$$T_{fi}^{BB (I=1)} = \frac{2^3 \pi \alpha_s}{3^2 \beta^2} \left[\frac{2^2}{3^{1/2}} {}_1F_1\left(1/2, 3/2; \frac{(\vec{A} - \vec{C})^2}{6\beta^2}\right) - {}_1F_1\left(1/2, 3/2; \frac{(\vec{A} - \vec{C})^2}{2\beta^2}\right) - 1 \right] e^{-(\vec{A} - \vec{C})^2 / 2\beta^2} + (\vec{C} \rightarrow -\vec{C}) . \quad (40)$$

This is the sum of Eqs.(26-29) for $\lambda = 1$, symmetrized as in Eq.(34). In this case there is an obvious partition into “direct meson” and “crossed meson” scattering contributions; the direct contributions have a forward-peaked Gaussian in $\vec{Q}^2 = (\vec{A} - \vec{C})^2$. Since the direct T_{fi} is a function only of \vec{Q}^2 no expansion in \vec{P}_i is required, and we obtain the potential simply by Fourier transforming;

$$V_{BB}^{(I=1)}(r) = \frac{1}{3^2 \pi^2} \frac{\alpha_s}{\beta^2} \int d^3 Q e^{i\vec{Q} \cdot \vec{x} - \vec{Q}^2 / 2\beta^2} \left\{ \frac{2^2}{3^{1/2}} {}_1F_1\left(1/2, 3/2; \frac{\vec{Q}^2}{6\beta^2}\right) - {}_1F_1\left(1/2, 3/2; \frac{\vec{Q}^2}{2\beta^2}\right) - 1 \right\} . \quad (41)$$

Evaluation of these integrals is discussed in App.B; the result is

$$V_{BB}^{(I=1)}(r) \Big|_{\text{color Coulomb}} = -\frac{2\alpha_s}{9r} \left[1 + (2/\pi)^{1/2} \beta r - 4 \text{Erf}(\beta r/2) \right] e^{-\beta^2 r^2 / 2} . \quad (42)$$

The three contributions in the square brackets are from T1, T2 and (C1+C2) respectively. The small- r behavior has an obvious interpretation; for $r \equiv r_{bb}$ much less than the wavefunction length scale β^{-1} , the Born-order heavy quark-quark interaction term T1 must approach the bare color Coulomb result $-2\alpha_s/9r$. The remaining quark-antiquark and antiquark-antiquark terms retain mean constituent separations of $O(\beta^{-1})$ as $r \rightarrow 0$ and so have nonsingular limits.

2. Spin-Spin Hyperfine

In the limit of large quark mass only the T2 diagram has a nonzero T_{fi} with this interaction, which for I=1 BB is given by Eq.(25) with $\lambda = 1$. Since this is a simple Gaussian, the $V_{BB}(r)$ resulting from Eq.(39) is also a Gaussian,

$$V_{BB}^{(I=1)}(r) \Big|_{\text{spin-spin hyperfine}} = + \frac{2^{1/2}}{9\pi^{1/2}} \frac{\alpha_s \beta^3}{\bar{m}^2} e^{-\beta^2 r^2/2} . \quad (43)$$

3. Linear Confinement

The T-matrix elements of the linear confining interaction for I=1 BB are given by Eqs.(30-33). In the $\lambda = 1$ large quark mass limit the forward-peaked part of T_{fi} equals

$$T_{fi} \Big|_{\text{direct}} = \frac{4\pi b}{3\beta^4} \left[-3^{1/2} {}_1F_1(-1/2, 3/2, \frac{\vec{Q}^2}{6\beta^2}) + {}_1F_1(-1/2, 3/2, \frac{\vec{Q}^2}{2\beta^2}) + 1 \right] e^{-\vec{Q}^2/2\beta^2} . \quad (44)$$

Evaluation of the Fourier transform of this T_{fi} requires an integral which is discussed in App.B. The result for $V_{BB}(r)$ is

$$V_{BB}^{(I=1)}(r) \Big|_{\text{lin. conf.}} = \frac{b}{6\beta} \left\{ \left[\beta r e^{-\beta^2 r^2/2} \right] + \left[2^{3/2} \frac{e^{-\beta^2 r^2/2}}{\pi^{1/2}} \right] + \left[- \left(\beta r + \frac{2}{\beta r} \right) \text{Erf}(\beta r/2) e^{-\beta^2 r^2/2} - 2 \frac{e^{-3\beta^2 r^2/4}}{\pi^{1/2}} \right] \right\} . \quad (45)$$

We have again grouped terms according to diagram. The first square bracket gives the T1 (quark-quark) term, the second is T2 (antiquark-antiquark), and the third is the rather complicated C1+C2 quark-antiquark term.

As with the Coulomb overlap integrals we could have anticipated some properties of this potential. First, at small r the interaction of two heavy quarks approaches the bare $V_{bb}(r_{bb})$ times a color and spin factor of 2/9 (instead of the usual $q\bar{q}$ color-singlet coefficient 4/3). Thus the T1 potential approaches $((2/9)/(4/3)) \cdot br = br/6$ for $r \ll \beta^{-1}$. The antiquark-antiquark (T2) and quark-antiquark (C1+C2) potentials again approach finite limits at small r , and give a contact potential of

$$V_{BB}^{(I=1)}(r=0)\Big|_{\text{lin. conf.}} = \frac{b}{6\beta} \left\{ \left[\frac{2^{3/2}}{\pi^{1/2}} \right] + \left[-\frac{4}{\pi^{1/2}} \right] \right\}. \quad (46)$$

The largest *individual* diagram contribution at contact is the positive T2 (antiquark-antiquark) term; the mean antiquark-antiquark separation is larger than quark-antiquark, which gives a larger linear-potential matrix element. However there are two contributing quark-antiquark diagrams, C1 and C2, which give equal contributions; their sum is larger than T2 and opposite in sign, so at contact we find a net attraction. At larger r the sign of this interaction is reversed.

C. $V_{BB}^{(I)}(r)$ final results

The full I=1 BB potential is given by

$$\begin{aligned} V_{BB}^{(I=1)}(r) = & -\frac{2\alpha_s}{9r} \left\{ 1 + (2/\pi)^{1/2} \beta r - 4 \text{Erf}(\beta r/2) \right\} e^{-\beta^2 r^2/2} + \frac{2^{1/2}}{9\pi^{1/2}} \frac{\alpha_s \beta^3}{\bar{m}^2} e^{-\beta^2 r^2/2} \\ & + \frac{b}{6\beta} \left\{ \beta r e^{-\beta^2 r^2/2} + \frac{2^{3/2}}{\pi^{1/2}} e^{-\beta^2 r^2/2} - \left(\beta r + \frac{2}{\beta r} \right) \text{Erf}(\beta r/2) e^{-\beta^2 r^2/2} - \frac{2}{\pi^{1/2}} e^{-3\beta^2 r^2/4} \right\}, \end{aligned} \quad (47)$$

which is the sum of the color Coulomb, OGE spin-spin and linear confinement contributions.

The potentials for the remaining \mathcal{BB} potentials can be obtained similarly. In all cases we find that for I=0 there is a simple relative flavor factor which changes the overall sign of $V_{\mathcal{BB}}$, as in Eq.(36). The various B^*B^* potentials can be determined from V_{BB} above by changing spin overlap matrix elements, which are given in Table II. For example, to convert the $V_{BB}^{(I=1)}(r)$ potential in Eq.(47) to $V_{B^*B^*}^{(I=1, S_{tot}=2)}(r)$ one multiplies the color Coulomb and linear contributions by $(+1)/(+1/2)$, and the remainder, the spin-spin hyperfine term ($\propto \alpha_s/\bar{m}^2$), by $(+1/4)/(+3/8)$.

The BB^* potentials require more careful treatment. Just as we found in BB , the BB^* T-matrix has forward- and backward-peaked contributions, but they are no longer

TABLE II. $I_{tot} = 1$ \mathcal{BB} Spin Matrix Elements (from Table I of [7]).

System		Operator	
mesons	S_{tot}	$\mathcal{O} = I$	$\mathcal{O} = \vec{S}_a \cdot \vec{S}_b$
BB	0	+1/2	+3/8
$BB^* \rightarrow BB^*$	1	+1/2	+3/8
$BB^* \rightarrow B^*B$	1	+1/2	-1/8
B^*B^*	2	+1	+1/4
	1	0	+1/2
	0	-1/2	+5/8

identical in magnitude; this was required for BB by Bose symmetry at the meson level. It is again useful to associate these with a “direct” $BB^* \rightarrow BB^*$ potential (from the forward-peaked contributions to the T-matrix) and a “crossed” $BB^* \rightarrow B^*B$ potential from the backward-peaked contribution, in which there is a $B \leftrightarrow B^*$ transition at each “crossed-V” interaction. At Born order in S-wave scattering the direct- and crossed-potentials can just be added to give a total effective BB^* potential. This total S-wave BB^* potential has twice the BB Coulomb and linear potential and $+2/3$ of the BB spin-spin potential, which makes it identical to the $S_{tot} = 2$ B^*B^* potential. The spin matrix elements for the direct and crossed BB^* contributions are given in Table II.

IV. DISCUSSION

A. Numerical results for $V_{BB}^{(I=1)}(r)$

We show the total $V_{BB}^{(I=1)}(r)$ of Eq.(47) and the three individual contributions in Fig.3. The parameters employed are $\alpha_s = 0.5$, $b = 0.18 \text{ GeV}^2$ and $\bar{m} = 0.33 \text{ GeV}$, which were used by Scora and Isgur in their recent HQET discussion of \mathcal{B} meson semileptonic

decays [13]. They quote several values of the variational best-fit SHO β for \mathcal{B} mesons, specifically $\beta = 0.43$ GeV (B), 0.40 GeV (B^*) and 0.35 GeV (1P B_J mesons); we adopt an intermediate value of 0.40 GeV.

The total I=1 BB quark model potential is evidently strongly attractive at small r , passes through a node at $r \approx 0.28$ fm, and is weakly repulsive at larger r . The Coulomb, spin-spin hyperfine and linear confinement contributions to $V_{BB}^{(I=1)}(r)$ for $r \approx 0.5$ -1 fm are all repulsive and are comparable in magnitude.

The short-range attraction is dominantly due to the color Coulomb attraction; for $r \ll \beta^{-1}$ the bound-state wavefunctions are irrelevant, and we see an unscreened color Coulomb potential between the heavy quarks, with a color-spin factor of $2/9$. This gives an attractive short distance potential $V_{bb}(r) = -2\alpha_s/9r$. At small r this quark-quark interaction diagram T1 is dominant; at larger r the other color Coulomb diagrams and bound state screening become important, and the Coulomb contribution crosses over to a weak repulsion at $r \approx 0.36$ fm. The Coulomb contribution is $+8$ MeV at 0.5 fm, and by 1 fm it has fallen to $+2$ MeV.

Of course at sufficiently small r the OGE Born approximation will be inaccurate, and the $bb\bar{q}\bar{q}$ system will deform to minimize the dominant small- r color Coulomb interaction. In I=1 the most attractive channel has bb in a color $\bar{3}$; this should give a stronger color Coulomb force than our Born result, and with these deformed wavefunctions our Born-order relation $V^{(I=0)} = -V^{(I=1)}$ will not be accurate.

The contribution of the linear confining interaction to $V_{BB}^{(I=1)}(r)$ is not large because there are approximate cancellations between the four diagrams and (unlike Coulomb) there is no regime in r in which one diagram dominates. We find that the linear contribution to $V_{BB}^{(I=1)}$ is attractive at short distances, with a contact value of about -50 MeV, and crosses over to a weak repulsion at $r \approx 0.38$ fm. At 0.5 fm the linear confining term contributes $+7$ MeV and at 1 fm it is $+6$ MeV.

In light-quark hadrons such as I=2 $\pi\pi$ and NN (the core potentials) one finds that

the color spin-spin hyperfine term makes the dominant contribution to the hadron-hadron interaction. Here we instead find that at moderate r the hyperfine, linear and Coulomb potentials make comparable contributions. The smaller hyperfine contribution to the BB system follows from the absence of both capture diagrams and one transfer diagram; these vanish due to the $1/m_i m_j$ prefactor in H_I Eq.(1). The spin-spin capture diagrams in particular made the largest contribution to the $I=2$ $\pi\pi$ interaction. We find that the hyperfine contribution to $V_{BB}^{(I=1)}(r)$ is repulsive (as in $I=2$ $\pi\pi$), but is much smaller; the contribution to $V_{BB}^{(I=1)}(r=0)$ is +26 MeV, which falls to +16 MeV at $r=0.5$ fm and +3 MeV at $r=1$ fm.

B. Comparison to LGT \mathcal{BB} potentials

Several references have discussed the determination of \mathcal{BB} potentials using LGT techniques [1–6]. The most detailed study to date is by the UKQCD collaboration [6]. This work treats the b quark as a static, spinless source, so there are four potentials, labelled by the light antiquarks' total isospin and spin, $(I_{tot}^{light}, S_{tot}^{light}) = (0, 0), (0, 1), (1, 0)$ and $(1, 1)$; these are shown in Figs.6-9 of Ref. [6]. Both $(0, 0)$ and $(1, 1)$ show strong short-range attraction. $(1, 1)$ appears consistent with weak repulsion beyond contact (the first lattice point is at $r \approx 0.18$ fm). The $(0, 0)$ potential shows a clear rise to a (probable) zero near 0.3 fm, and some evidence for weak repulsion at larger r . The $(1, 0)$ and $(0, 1)$ potentials are small (*ca.* ± 50 MeV) and are not yet well characterized, although $(0, 1)$ shows some intermediate-range attraction, and both potentials show evidence of repulsion at contact.

Comparison of our quark model \mathcal{BB} potentials to these LGT results is unfortunately nontrivial except for $S_{tot} = 2 B^* B^*$, due to the spin degree of freedom. The lattice static-quark limit has degenerate B and B^* mesons, so the lowest-energy configuration for given S_{tot}^{light} will not be the external source basis state (such as $|BB\rangle$, as in our quark model calculation) but instead will be the linear superposition of $|BB\rangle$, $|BB^*\rangle$ and $|B^*B^*\rangle$ that gives the lowest expected energy [14].

A direct comparison does appear possible for the UKQCD $S_{tot}^{light} = 1$ potentials, which correspond to an $S_{tot} = 2 B^* B^*$ meson pair. These have no S-wave degenerate BB or $B^* B^*$ mixing states, and should therefore be similar in physical meaning to our $S_{tot} = 2 B^* B^*$ quark model potentials, provided that the tensor coupling to L=2 BB is unimportant. In Figs.4,5 we compare the (1,1) and (0,1) LGT potentials to our I=1,0 $S_{tot} = 2 B^* B^*$ potentials. Clearly there is qualitative similarity, although the quark model potentials appear to have a larger length scale.

A more realistic comparison is possible if we apply an estimated lattice resolution effect “smearing” to our quark model potential. Lattice resolution can have a dramatic effect on some aspects of the potential, especially near $r = 0$ where there is little Jacobean weight. For example it will regularize a continuum $1/r$ term, so that the LGT \mathcal{BB} potentials approach finite values at contact, as noted by Stewart and Koniuk [4]. To model lattice resolution effects we introduce a Gaussian-averaged quark model potential, defined by

$$\tilde{V}(r) = \int d^3\mathbf{r}' \frac{1}{\pi^{3/2}a^3} \exp\{-(\mathbf{r} - \mathbf{r}')^2/a^2\} V(r') . \quad (48)$$

We choose the smearing length a to be the lattice resolution of 0.18 fm estimated by UKQCD for their LGT results [6]. The resulting \tilde{V} potentials are shown as dashed lines in Figs.4,5. Except for what appears to be a difference in the length scale, these are qualitatively similar to the LGT potential. In future we should ideally compare with LGT potentials from simulations that have a finer spatial resolution.

The isospin dependence of the quark model \mathcal{BB} potentials is a very characteristic feature. The I=0 Born-order quark model potentials are equal in magnitude but opposite in sign to the I=1 potentials. This result *may* be supported by LGT at intermediate r (compare the LGT (0,0) with $-(1,0)$ and (0,1) with $-(1,1)$ in [6]); (0,1) and (1,1) are also shown in our Figs.4,5. At contact however the LGT I=0 and I=1 results differ greatly in magnitude; since I=0 is odd- L it may be difficult to extract the small- r I=0 BB potential, and in any case we expect the Born result to be inaccurate at small r , because the strong color Coulomb term will dominate.

C. Bound States

Bound meson pairs, known as “molecules”, most easily form in channels in which the pair can exist in S-wave. From Table I the S-wave \mathcal{BB} channels are $I=1 BB$, $I=0,1 BB^*$, and $(I, S_{tot}) = (1, 0), (0, 1)$ and $(1, 2) B^*B^*$. We have searched for possible bound states in these \mathcal{BB} and \mathcal{DD} systems by numerically integrating the two-meson Schrödinger equation with the generalizations of Eq.(47) to the different spin channels.

With our standard parameter set (in Sec.IV.A) and assuming B and B^* masses of 5.288 GeV and 5.325 GeV, we find that only one channel has sufficient attraction to form a bound state; this is $I=0 BB^*$, which has a deuteron-like repulsive core and intermediate-range attraction. We find a binding energy of just -5.5 MeV with our parameters, typical of nuclear binding energies.

The most attractive of the $I=1$ attractive-core channels are BB^* and $S_{tot} = 2 B^*B^*$, which have identical potentials. The attraction however is not strong enough to overcome the intermediate-range repulsion. As we increase α_s we do find that these systems bind, but at an unphysical $\alpha_s \approx 1.0$, about twice the usual quark-model value.

In all the \mathcal{DD} channels the smaller reduced mass makes binding more difficult, and we find no bound states.

One pion exchange forces are often suggested as an important component of the meson-meson interaction, and have been discussed in general by Törnqvist [15] and quantitatively by Ericson and Karl [16]. Ericson and Karl find that one pion exchange is not attractive enough to bind mesons lighter than \mathcal{BB} , but that the $I=0 S_{tot} = 2$ (odd-L) B^*B^* channel will bind from this interaction alone. The S-wave \mathcal{BB} channels with attractive one pion exchange forces are $I=1 S_{tot} = 0 B^*B^*$ [15] and $I=0 BB^*$ [17]. Since we expect both one pion exchange and quark-gluon forces to be present in nature, one might study the combined effect of the one pion exchange potential and the analogues of our Eq.(47) in a search for bound states in other channels that are more accessible to experiment than \mathcal{BB} .

V. CONCLUSIONS

We have calculated the T-matrix and low energy equivalent potentials between pairs of heavy-light mesons, the “ \mathcal{BB} ” system, in the context of the nonrelativistic quark model. The assumed scattering mechanism is a single interaction of the standard quark model Hamiltonian, with OGE color Coulomb and spin-spin terms and linear confinement. The parameters used were taken from previous studies of meson spectroscopy and HQET matrix elements. This model of the hadron-hadron T-matrix is known from previous work to give a good description of experiment in the analogous light pseudoscalar channels $I=2$ $\pi\pi$ and $I=3/2$ $K\pi$. We carry out the overlap integrals of this interaction with standard SHO external $b\bar{q}$ meson wavefunctions in closed form, and so obtain analytic results for $V_{\mathcal{BB}}^{(I=0,1)}(r)$ in the various allowed channels. These are compared to recent LGT results from the UKQCD collaboration in the channels where this is possible, which are $I=0,1$, $S_{tot} = 2 B^*B^*$. We find results similar to these UKQCD potentials after lattice smearing, but with a somewhat larger length scale. Our $I=1$ BB potential however is attractive at small r , which appears inconsistent with UKQCD results.

We find that our quark model potentials are sufficiently attractive to support a bound state in only one channel, $I=0$ BB^* , which has a deuteron-like potential. With pion exchange added, other channels may have sufficient attraction to support bound states.

In future work a more detailed comparison with LGT potentials, especially below 0.2 fm, will be important as a test of the forces assumed in the quark model calculation. It would also be very interesting to generate LGT \mathcal{BB} potentials for large but finite quark mass, so the meson spins could be specified uniquely. One could then compare the LGT and phenomenological \mathcal{BB} potentials in all channels unambiguously. Finally, one may extract the spin-dependent (spin-orbit, spin-spin, tensor and so forth) equivalent \mathcal{BB} meson channels using similar techniques, and we anticipate that a comparison with LGT results for these potentials might also be interesting as a test of the nature of spin-dependent “nuclear” forces.

VI. ACKNOWLEDGEMENTS

We would like to thank N.Isgur, G.Karl, R.Koniuk, C.Michael, P.Pennanen and S.R.Sharpe for useful discussions. This work was supported in part by the USDOE under Contract No. DE-FG02-96ER40947 managed by North Carolina State University and under Contract No. DE-AC05-96OR22464 managed by Lockheed Martin Energy Research Corp.

APPENDIX A: MESON WAVEFUNCTIONS

In this appendix we present the explicit meson wavefunctions used in the paper. A single meson state is given by

$$|A(\vec{A}, S, S_z)\rangle = \sum_{c, \bar{c}=1}^3 \frac{1}{\sqrt{3}} \delta_{c\bar{c}} \sum_{s_z, \bar{s}_z} \langle S, S_z | 1/2, s_z; 1/2, \bar{s}_z \rangle \iint d^3a d^3\bar{a} \delta(\vec{A} - \vec{a} - \vec{\bar{a}}) \Phi_A(\vec{a}_{rel}) |q_{\bar{a}s_z}^c \bar{q}_{\vec{a}\bar{s}_z}^{\bar{c}}\rangle, \quad (\text{A1})$$

where the relative momentum variable is $\vec{a}_{rel} = (\bar{m}\vec{a} - m\vec{\bar{a}})/((m + \bar{m})/2)$. The full momentum-space wavefunction is

$$\Phi_A(\vec{A}, \vec{a}, \vec{\bar{a}}) = \delta(\vec{A} - \vec{a} - \vec{\bar{a}}) \Phi_A(\vec{a}_{rel}) \quad (\text{A2})$$

We normalize this state to

$$\langle A(\vec{A}, S, S_z) | A(\vec{A}', S', S'_z) \rangle = \delta(\vec{A} - \vec{A}') \delta_{SS'} \delta_{S_z S'_z}, \quad (\text{A3})$$

and the individual quark and antiquark states are similarly normalized as

$$\langle q(\vec{a}, s, s_z) | q(\vec{a}', s'_z) \rangle = \delta(\vec{a} - \vec{a}') \delta_{s s'_z}. \quad (\text{A4})$$

This implies a relative-momentum wavefunction normalization of

$$\int d^3(a_{rel}/2) |\Phi_A(\vec{a}_{rel})|^2 = 1. \quad (\text{A5})$$

The full and relative spatial wavefunctions are related by

$$\Psi_A(\vec{x}_{cm}, \vec{r}) = \frac{e^{+i\vec{p}_{cm}\cdot\vec{x}_{cm}}}{(2\pi)^{3/2}} \psi_A(\vec{r}) \quad (\text{A6})$$

with $\vec{x}_{cm} = (m\vec{x}_q + \bar{m}\vec{x}_{\bar{q}})/(m + \bar{m})$ as usual. These are related to the momentum-space wavefunctions by

$$\Phi_A(\vec{A}, \vec{a}, \vec{\bar{a}}) = \frac{1}{(2\pi)^3} \iint d^3x_{cm} d^3r e^{-i(\vec{a}+\vec{\bar{a}})\cdot\vec{x}_{cm} - i\vec{\bar{a}}_{rel}\cdot\vec{r}/2} \Psi_A(\vec{x}_{cm}, \vec{r}) . \quad (\text{A7})$$

The relative spatial wavefunction $\psi_A(\vec{r})$ is similarly related to the relative momentum wavefunction Φ_A by

$$\psi_A(\vec{r}) = \frac{1}{(2\pi)^{3/2}} \int d^3(a_{rel}/2) e^{+i(\vec{a}_{rel}/2)\cdot\vec{r}} \Phi_A(\vec{a}_{rel}) , \quad (\text{A8})$$

where $\vec{r} = \vec{x}_q - \vec{x}_{\bar{q}}$.

The ground state SHO quark model wavefunction which we use in the potential calculations discussed in the text is

$$\Phi_A(\vec{a}_{rel}) = \Phi_0(\vec{a}_{rel}) = \frac{1}{\pi^{3/4} \beta^{3/2}} \exp \left\{ -\vec{a}_{rel}^2 / 8\beta^2 \right\} . \quad (\text{A9})$$

APPENDIX B: OVERLAP INTEGRALS

In deriving \mathcal{BB} potentials as Fourier transforms of the scattering amplitudes we encountered shifted-Gaussian overlap integrals of the form

$$I_{a,c} \equiv \int d^3Q e^{-c_0\vec{Q}^2/\beta^2 + i\vec{Q}\cdot\vec{r}} {}_1F_1(a, c; c_1 \frac{\vec{Q}^2}{\beta^2}) . \quad (\text{B1})$$

To evaluate integrals of this type it is useful to introduce an integral representation of the confluent hypergeometric function. For $c > a > 0$ we use

$${}_1F_1(a, c; x) = \frac{\Gamma(c)}{\Gamma(a)\Gamma(c-a)} \int_0^1 dt e^{xt} t^{a-1} (1-t)^{c-a-1} \quad (\text{B2})$$

which leads to

$$I_{a,c} = \frac{\Gamma(c)}{\Gamma(a)\Gamma(c-a)} \left(\frac{\pi}{c_0}\right)^{3/2} \beta^3 \frac{c_0^a}{c_1^{c-1}} (c_0 - c_1)^{c-a-1} e^{-\rho} \int_0^k dy y^{a-1} (y+1)^{3/2-c} (k-y)^{c-a-1} e^{-\rho y} \quad (\text{B3})$$

where $k = (c_0/c_1 - 1)^{-1}$ and $\rho = \beta^2 r^2 / 4c_0$. For the color Coulomb interaction we have $c = 3/2$ and $c = a + 1$, so the integral becomes

$$I_{1/2,3/2} = \int d^3Q e^{-c_0 \vec{Q}^2 / \beta^2 + i\vec{Q} \cdot \vec{r}} {}_1F_1(1/2, 3/2; c_1 \frac{\vec{Q}^2}{\beta^2}) = \frac{\pi^{3/2} \beta^3}{2c_0^2 c_1^{1/2}} \frac{e^{-\rho}}{\rho^{1/2}} \int_0^{k\rho} ds s^{-1/2} e^{-s} = \frac{\pi^2 \beta^2}{r} (c_0 c_1)^{-1/2} e^{-\beta^2 r^2 / 4c_0} \text{Erf}(c_2 \beta r) \quad (\text{B4})$$

where $c_2 = c_0^{-1/2} (c_0/c_1 - 1)^{-1/2} / 2$. The special case $c_0 = c_1$ is

$$I_{1/2,3/2} \Big|_{c_0=c_1} = \frac{\pi^2 \beta^2}{c_0 r} e^{-\beta^2 r^2 / 4c_0} . \quad (\text{B5})$$

The linear confinement overlap integrals lead to the case $a = -1/2$ and $c = 3/2$. The required integral is

$$I_{-1/2,3/2} = \int d^3Q e^{-c_0 \vec{Q}^2 / \beta^2 + i\vec{Q} \cdot \vec{r}} {}_1F_1(-1/2, 3/2; c_1 \frac{\vec{Q}^2}{\beta^2}) = \frac{\pi^2 \beta^3}{2} \frac{c_1^{1/2}}{c_0^2} e^{-\beta^2 r^2 / 4c_0} \left\{ (c_0/c_1 - 1)^{1/2} \left(u + \frac{1}{2u}\right) \text{Erf}(u) - \frac{(2c_0/c_1 - 1)}{(c_0/c_1 - 1)^{3/2}} \frac{e^{-u^2}}{\pi^{1/2}} \right\} + \frac{\pi^{3/2} \beta^3}{2(c_0 - c_1)^{3/2}} e^{-\beta^2 r^2 / 4(c_0 - c_1)} \quad (\text{B6})$$

and the special case $c_0 = c_1$ is

$$I_{-1/2,3/2} \Big|_{c_0=c_1} = \frac{\pi^2 \beta^4}{4c_0^2} r e^{-\beta^2 r^2 / 4c_0} . \quad (\text{B7})$$

-
- [1] D.Richards, D.Sinclair and D.Sivers, Phys. Rev. D42, 3191 (1990).
- [2] A.Mihaly, H.R.Fiebig, H.Markum and K.Rabitsch, Phys. Rev. D55, 3077 (1997).
- [3] H.R.Fiebig, H.Markum, A.Mihaly, K.Rabitsch and R.M.Woloshyn, hep-lat/9709152, Nucl. Phys. Proc. Suppl. 63, 188 (1998).
- [4] C.Stewart and R.Koniuk, hep-lat/9803003, Phys. Rev. D57, 5581 (1998).
- [5] C.Michael (UKQCD Collaboration), hep-ph/9809211, in Proceedings of “*Confinement III*” (CEBAF, June 1998).
- [6] C.Michael and P.Pennanen (UKQCD Collaboration), hep-lat/9901007 (Jan. 1999).
- [7] T.Barnes and E.S.Swanson, Phys. Rev. D46, 131 (1992); see also G.-Q.Zhao, X.G.Jing and J-C.Su, Phys. Rev. D58, 117503-1 (1998) ($\pi\pi$ scattering); D.Blaschke and G.Röpke, Phys. Lett. B299, 332 (1993) and K.Martins, D.Blaschke and E.Quack, Phys. Rev. C51, 2723 (1995) ($c\bar{c}$ propagation in media).
- [8] E.S.Swanson, Ann. Phys. (N.Y.) 220, 73 (1992).
- [9] T.Barnes, E.S.Swanson and J.Weinstein, Phys. Rev. D46, 4868 (1992).
- [10] T.Barnes and E.S.Swanson, Phys. Rev. C49, 1166 (1994).
- [11] There is an extensive literature on quark model calculations of the NN force, beginning with D.A.Liberman, Phys. Rev. D16, 1542 (1977). More recent studies have employed resonating group methods (see for example C.S.Warke and R.Shanker, Phys. Rev. C21, 2643 (1980); M.Oka and K.Yazaki, Phys. Lett. 90B, 41 (1980); C.S.Warke and R.Shanker, Phys. Rev. C21, 2643 (1980); J.E.T.Ribeiro, Z.Phys.C5, 27 (1980)) and variational methods (for example K.Maltman and N.Isgur, Phys. Rev. D29, 952 (1984)). A more extensive set of references and the Born-order OGE NN results analogous to the present paper are given in

- T.Barnes, S.Capstick, M.D.Kovarik and E.S.Swanson, Phys. Rev. C48, 539 (1993).
- [12] T.Barnes and G.I.Ghandour, Phys. Lett. B118, 411 (1982), give a systematic procedure for converting a general T-matrix into an equivalent potential operator.
- [13] D.Scora and N.Isgur, Phys. Rev. D52, 2783 (1995); see esp. App.A.
- [14] For this reason it appears plausible that the LGT $V_{\mathcal{B}\mathcal{B}}$ in the $S_{tot}^{light} = 0$ sector might be a lower bound for the true V_{BB} . If this is the case our quark model $V_{BB}^{(I=1)}(r)$, which is strongly attractive at small r , disagrees with the UKQCD lower bound, which suggests no short-range attraction. (Compare our Fig.3 with the presumed lower bound provided by Fig.8 of [6].) The actual comparison may be more complicated, however, because short-range attraction appears unavoidable in this channel. At very small r_{bb} the bb system will find it energetically favorable to rearrange into a color $\bar{3}$, which gives an attractive bb color Coulomb contribution of $V_{bb} = -2\alpha_s/3r$. The spectator light antiquarks should not significantly modify this conclusion.
- [15] N.A.Törnqvist, Phys. Rev. Lett. 67, 556 (1991).
- [16] T.E.O.Ericson and G.Karl, Phys. Lett. B309, 426 (1993).
- [17] G.Karl, private communication.

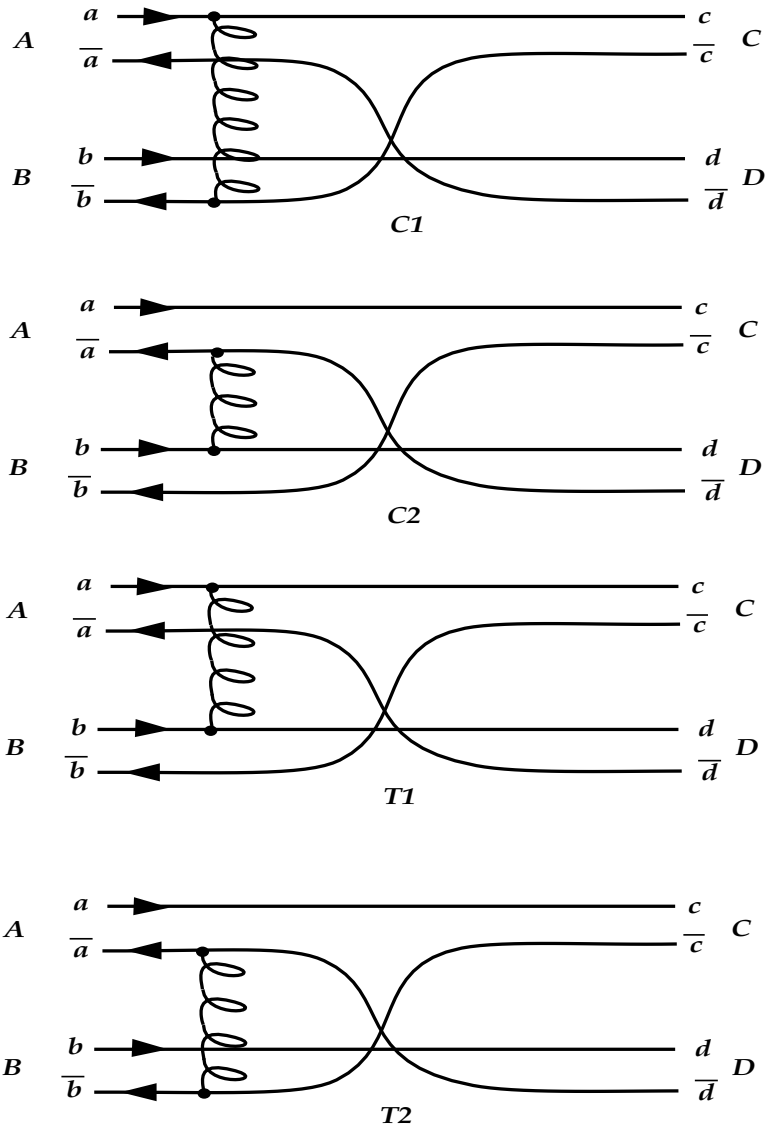


Fig.1. The four meson-meson scattering diagrams.

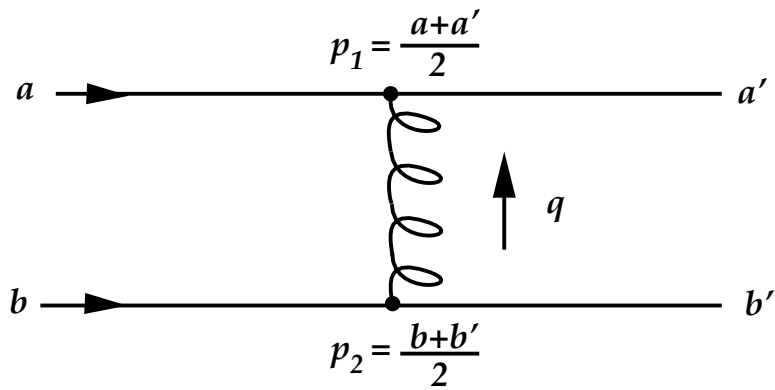


Fig.2. Momentum definitions in the quark-quark T-matrix element.

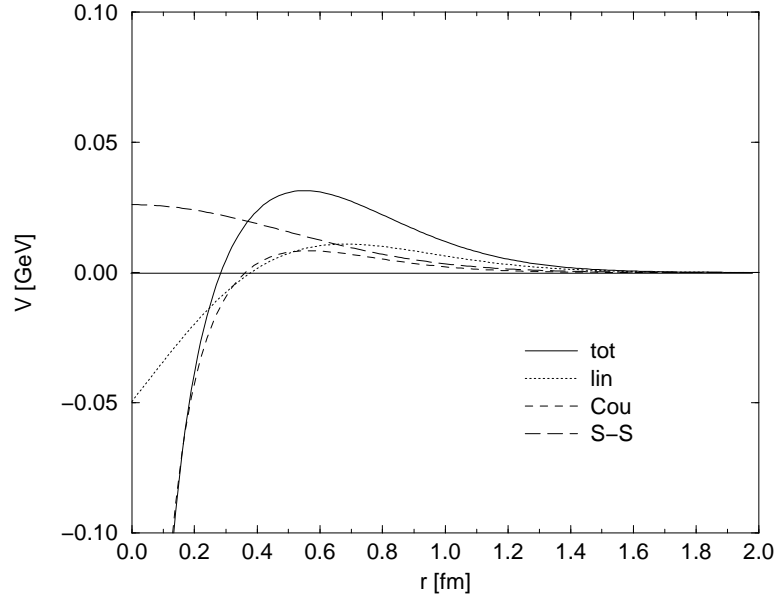


Fig.3. The $V_{BB}^{(I=1)}$ potential, showing individual contributions.

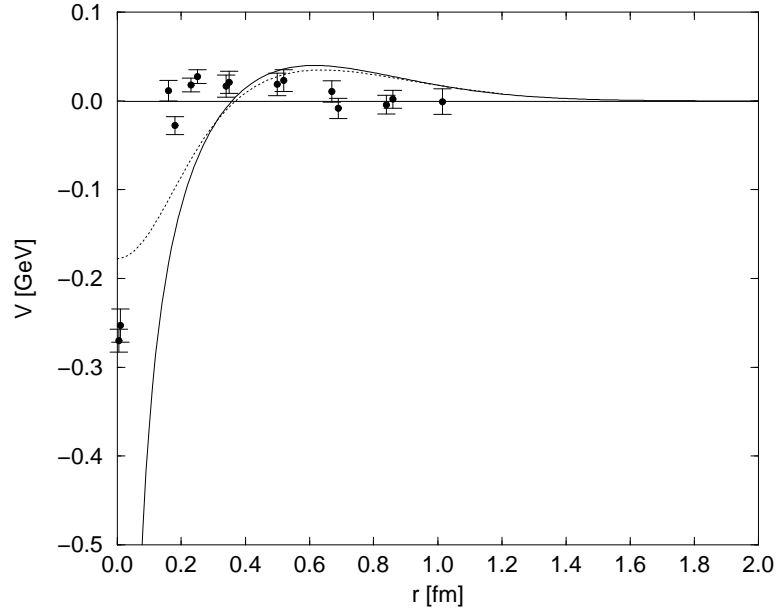


Fig.4. Comparison of the $V_{B^*B^*}^{(I=1, S_{tot}=2)}$ quark model potential (solid is calculated, dashed is smeared by $a = 0.18$ fm) with the $V_{BB}^{(I_{light}=1, S_{light}=1)}$ LGT potential of Ref. [6].

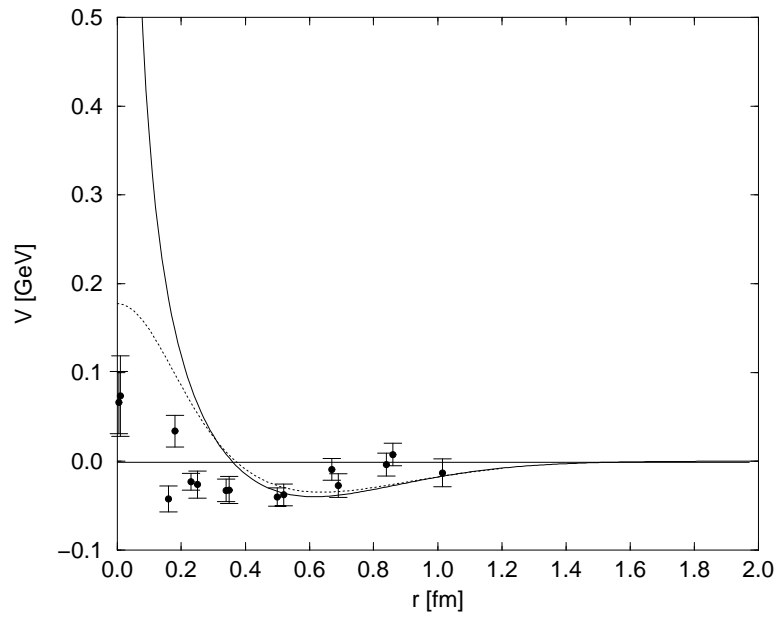


Fig.5. Comparison of the $V_{B^*B^*}^{(I=0, S_{tot}=2)}$ quark model potential (solid is calculated, dashed is smeared by $a = 0.18$ fm) with the $V_{BB}^{(I_{light}=0, S_{light}=1)}$ LGT potential of Ref. [6].